International Journal of Computational Methods
Vol. 8, No. 4 (2011) 637–651

DOI: 10.1142/S0219876211002733

World Scientific
www.worldscientific.com

MODELING OF CONTACT ANGLES AND WETTING EFFECTS WITH PARTICLE METHODS

M. B. LIU*

Key Laboratory for Hydrodynamics and Ocean Engineering
Institute of Mechanics
Chinese Academy of Sciences
Beijing 100190, China

The State Key Laboratory for Nonlinear Mechanics
Institute of Mechanics
Chinese Academy of Sciences
Beijing 100190, China
liumoubin@imech.ac.cn

J. Z. CHANG†, H. T. LIU and T. X. SU

School of Mechatronice Engineering
North University of China
Taiyuan, 030051, China
†*changjz01@nuc.edu.cn*

Received 16 November 2009
Accepted 16 August 2010

The physics of fluid–fluid–solid contact line dynamics and wetting behaviors are closely related to the inter-particle and intra-molecular hydrodynamic interactions of the concerned multiple phase system. Investigation of surface tension, contact angle, and wetting behavior using molecular dynamics (MD) is practical only on extremely small time scales (nanoseconds) and length scales (nanometers) even if the most advanced high-performance computers are used. In this article we introduce two particle methods, which are smoothed particle hydrodynamics (SPH) and dissipative particle dynamics (DPD), for multiphase fluid motion on continuum scale and meso-scale (between the molecular and continuum scales). In both methods, the interaction of fluid particles and solid particles can be used to study fluid–fluid–solid contact line dynamics with different wetting behaviors. The interaction strengths between fluid particles and between fluid and wall particles are closely related to the wetting behavior and the contact angles. The effectiveness of SPH and DPD in modeling contact line dynamics and wetting behavior has been demonstrated by a number of numerical examples that show the complexity of different multiphase flow behaviors.

Keywords: Contact angles; wetting and non-wetting; particle methods; smoothed particle hydrodynamics (SPH); dissipative particle dynamics (DPD).

*Corresponding author.

1. Introduction

The behavior of multiphase fluids in contact with solid surfaces is important in almost all areas of science and technology including nuclear reactor heat exchangers, lubricated pipeline transport, manufacturing of multilayer films and fibers, chemical reactors and separators, coating systems, enhanced oil and gas production, and environmental remediation [De Gennes (1985); Bracke *et al.* (1989)]. One frequently observable yet physically complex example is the attachment of a liquid drop onto a solid surface. Depending on the physical nature of the concerned fluids and solids, the liquid drop can display different wetting behavior: filming, spreading, and maintaining a nearly circular liquid drop. For simple solid surfaces or complex solid grains (such as finely designed structures and randomly distributed porous rocks), the liquid may behave as a paint, a lubricant, an ink, or a dye.

Modeling of contact line dynamics (in fact, contact point dynamics in 2D and contact line dynamics in 3D) and wetting behavior with conventional grid-based numerical methods is usually fraught with difficulties, especially when treating geometrically complex boundaries, fluid–fluid–solid contact line dynamics, and fluid–fluid interface dynamics, conventional Eulerian-grid-based numerical methods such as FDM and FVM require special algorithms to treat and track moving interfaces and usually lead to artificially broadened interfaces. On the other hand, Lagrangian-grid-based methods such as FEM have problems in dealing with large flow deformation and usually lead to mesh entanglement [Liu *et al.* (2008)].

There is a growing interest in applying Lattice Boltzmann (LB) models to both single-phase and multiphase flow simulations [Rothman and Keller (1988); Shan and Chen (1993); Chen and Doolen (1998); Házi *et al.* (2002)]. In LB simulations, continuum hydrodynamics (quantitatively described by the Navier–Stokes equations) is replaced by micro-dynamic equations confined to a lattice via interactions between the fluid(s) and solid(s) on adjacent nodes. One problem is that, most LB models are only applicable to multiphase systems with low to moderate density and viscosity contrasts usually less than 10–100. In order to accurately model larger density contrasts (e.g., water/air density ratio is about 1000:1), further development of the LB method is required. Inamuro *et al.* [2004] developed an LB model that is able to handle large density ratio up to 1,000 without suffering from numerical instability. Although their results are very promising, the applicability of this new LB model to problems with large density and viscosity contrast still needs more rigorous comparisons with experimental observations or other well-validated numerical models. Another problem is that, due to the restriction of the dynamics to the streaming of "particles" between adjacent nodes on a regular lattice, the LB models are not always Galilean invariant.

Considering the fact that both fluids and solids are composed of particles (on atomistic/molecular scale, a particle may represent an atom or a molecule; on meso-scale, a particle may contain a cluster of atoms or molecules; and on continuum scale, a particle can stand for an infinitesimal volume of fluids or solids), the

physics of fluid–fluid–solid contact line dynamics as well as wetting behaviors are closely related to the inter-particle and intra-molecular hydrodynamics interactions of the concerned multiple phase system. By numerically integrating the equations of motion of the constitutive particles, the fluid property (either simple fluids or complex fluids), fluid–fluid interaction, and fluid–fluid–solid contact line dynamics as well as wetting behavior can be modeled. Conventional molecular dynamics (MD) [Frenkel and Smit (2002); Rapaport (2004)] is such a particle method on atomistic/molecular scale, and can be used for simulating single-phase and multiphase fluid dynamics [Thompson and Robbins (1989)] and liquid spreading with contact line dynamics [Wu *et al.* (2003)]. The MD is in principle capable of providing reliable results on all scales, but is yet restricted from practical applications due to the extremely small time scales (nanoseconds) and length scales (nanometers).

Another approach is to use off-lattice particle-based simulation methods, similar to MD. An individual particle represents a volume of fluid that may vary in size, depending on the model, from a small cluster of atoms or molecules on meso-scale, to a macroscopic region in a solid or fluid on continuum scale. These off-lattice particle-based methods exactly conserve mass and momentum, and are Galilean invariant (unlike some LB models). Dissipative particle dynamics (DPD) [Hoogerbrugge and Koelman (1992); Groot (1997)] and smoothed particle hydrodynamics (SPH) [Gingold and Monaghan (1977)] are such particle methods on meso and continuum scales, respectively. Here, we describe SPH and DPD models for modeling of contact angles and wetting effects with a number of exemplary numerical examples.

2. Contact Angles and Wetting Effects

On continuum scale, when a system consisting fluid–fluid–solid reaches equilibrium, the material interfaces can also arrive at equilibrium. The tangential lines of the fluid–fluid interface and fluid–solid interface form the contact angle. The continuum concept of a contact angle supposes that the visible fluid–fluid interface can be extrapolated to the solid surface and that the contact angle θ is related to the interfacial forces by (Fig. 1)

$$\sigma_{1S} - \sigma_{2S} = \sigma_{12}\cos\theta, \tag{1}$$

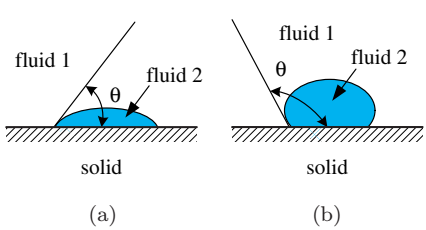

Fig. 1. Contact angle and wetting effects of a liquid drop attaching onto a solid surface: (a) wetting with an acute angle and (b) non-wetting with an obtuse angle.

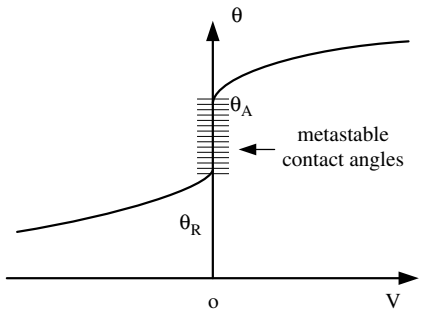

Fig. 2. Evolution of the contact angles with the contact line movement velocity V.

where σ_{1S} and σ_{1S} are the fluid–solid interfacial forces between fluid 1 (e.g. air) and solid and between fluid 2 (e.g. water) and solid. σ_{12} is the fluid–fluid interfacial force (surface tension). When $\theta < 90°$, the solid surface is wetted by fluid 2, and when $\theta \geq 90°$, the solid surface is not wetted by fluid 2. When the contact angle approaches zero, fluid 2 can form a thin film on the solid surface.

The above descriptions regarding the contact line dynamics are based on continuum assumptions that are not consistent with a molecular interpretation. On molecular scale, contact line dynamics can be much more complicated and is closely related to properties of the concerned fluids and solids and chemical and physical heterogeneities (impurities and surface roughness).

First, the properties of the fluid near the fluid–solid and fluid–fluid interfaces can deviate from the bulk properties and, therefore, the behavior of fluid particles next to the solid surface may not be well addressed by continuum concept. Second, impurities and surface roughness can lead to energy barriers that must be overcome when a fluid particle adjacent to the surface moves from one position from another. Third, the contact angles can be different for advancing fluids (advancing contact angle θ_{A}) and receding fluids (receding contact angle θ_{B}), and can vary with the movement of the contact line, due to the complexity of fluid–fluid and fluid–solid interactions, and chemical and physical heterogeneities. For many applications, there is a range of static contact angles when the contact line stays at a metastable state Fig. 2.

3. Smoothed Particle Hydrodynamics

SPH is a "truly" meshfree particle method originally invented to solve astrophysical problems in 3D open space, since the collective movement of those particles is similar to the movement of a liquid or gas flow, and it can be modeled by the governing equations of the classical Newtonian hydrodynamics. In SPH, the state of a system is represented by a set of particles, which possess material properties and interact with each other within the range controlled by a weight function or smoothing function [Liu and Liu (2003); Liu *et al.* (2003b)]. The discretization of the governing equations is based on these discrete particles and a variety of particle-based formulations

have been used to calculate the local density, velocity, and acceleration of the fluid. The fluid pressure is calculated from the density using an equation of state, the particle acceleration is then calculated from the pressure gradient and the density. For viscous flows, the effects of physical viscosity on the particle accelerations can also be included. In SPH, there is no explicit interface tracking for multiphase flows — the motion of the fluid is represented by the motion of the particles, and fluid surfaces or fluid–fluid interfaces move with particles representing their phase defined at the initial stage.

There have been a lot of literatures addressing the applications of SPH method to simulate multiphase contact line dynamics with surface tension, contact angle, and wetting effects. Nugent and Posch described an approach to modeling liquid drops and surface tension for a van der Waals (vdW) fluid [Nugent and Posch (2000)]. The cohesive pressure in the equation of state for the vdW fluid actually acts an attractive force among SPH particles. Liu *et al.* applied the SPH method to multiphase fluid flow in microchannels with applications to flip-chip underfill encapsulation process with both isotropic and anisotropic smoothing kernels [Liu *et al.* (2003a); Liu and Liu (2005)]. Li *et al.* proposed an SPH model for simulating droplet collision and coalescence [Li *et al.* (2006)]. Fang *et al.* also developed an SPH model for the simulations of droplet spreading and solidification [Fang *et al.* (2009)]. Tartakovsky and Meakin applied the SPH method to the modeling of surface tension and contact angle [Tartakovsky and Meakin (2005)].

In the SPH method, particles are employed to represent the state and record the movement of a system. A field function and its first derivative at a particle i can be numerically approximated as the summation over the nearest neighboring particles that are within the influence domain of particle i through a smoothing function W.

$$\langle f\rangle_i = \sum_{j=1}^{N}\left(\frac{m_j}{\rho_j}\right) f_j W_{ij}, \tag{2}$$

$$\langle \nabla\cdot f\rangle_i = \sum_{j=1}^{N}\left(\frac{m_j}{\rho_j}\right) f_j \cdot \nabla_i W_{ij}, \tag{3}$$

where, m_j and ρ_j are the mass and density of particle j. N is the total number of neighboring particles. Substituting the SPH approximations for a function and its derivative to the Navier–Stokes equation, the SPH equations of motion can be written as follows.

$$\begin{cases} \dfrac{D\rho_i}{Dt} = \displaystyle\sum_{j=1}^{N} m_j \mathbf{v}_{ij}^{\beta}\frac{\partial W_{ij}}{\partial \mathbf{x}_i^{\beta}} \\ \dfrac{D\mathbf{v}_i^{\alpha}}{Dt} = -\displaystyle\sum_{j=1}^{N} m_j\left(\frac{\sigma_i^{\alpha\beta}}{\rho_i^2}+\frac{\sigma_j^{\alpha\beta}}{\rho_j^2}\right)\frac{\partial W_{ij}}{\partial \mathbf{x}_i^{\beta}} + 2\gamma k(x_i)\left(\frac{m_i}{\rho_i}\right)\Delta\left(\frac{m_i}{\rho_i}\right), \\ \dfrac{De_i}{Dt} = \dfrac{1}{2}\displaystyle\sum_{j=1}^{N} m_j\left(\frac{p_i}{\rho_i^2}+\frac{p_j}{\rho_j^2}\right)\mathbf{v}_{ij}^{\beta}\frac{\partial W_{ij}}{\partial \mathbf{x}_i^{\beta}} + \frac{\mu_i}{2\rho_i}\varepsilon_i^{\alpha\beta}\varepsilon_i^{\alpha\beta} \end{cases} \tag{4}$$

where the scalar density ρ, internal energy e, the velocity component $\mathbf{v}^\alpha$, and the total stress tensor $\sigma^{\alpha\beta}$ are the dependent variables. The spatial coordinates $\mathbf{x}^\alpha$ and time t are the independent variables. α and β are Greek superscripts used to denote the coordinate directions and the summation in the equations is taken over repeated indices. The total stress tensor $\sigma^{\alpha\beta}$ is made up of two parts, one part of isotropic pressure p and the other part of viscous stress τ, i.e., $\sigma^{\alpha\beta} = -p\delta^{\alpha\beta} + \tau^{\alpha\beta}$. For Newtonian fluids, the viscous shear stress should be proportional to the shear strain rate denoted by ε through the dynamic viscosity μ, i.e., $\tau^{\alpha\beta} = \mu\varepsilon^{\alpha\beta}$, where $\varepsilon^{\alpha\beta} = \frac{\partial \mathbf{v}^\beta}{\partial \mathbf{x}^\alpha} + \frac{\partial \mathbf{v}^\alpha}{\partial \mathbf{x}^\beta} - \frac{2}{3}(\nabla \cdot \mathbf{v})\delta^{\alpha\beta}$.

There are basically two approaches to model multiphase contact line dynamics with SPH method. The first approach is to introduce an inter-particle interaction force (IIF) in the SPH equations, and can be termed as IIF model. The IIF can contain short-distance repulsion and long-range attraction, and the attractive force between every pair of SPH particles contribute to the surface tension. One IIF model is to directly apply an IIF in the SPH method, just as taken by Tartakovsky and Meakin as follows [Tartakovsky and Meakin (2005)]

$$\mathbf{F}_{ij} = s_{ij} \cos\left(\frac{1.5\pi}{kh}\right) \mathbf{r}_{ij}, \tag{5}$$

where s_{ij} is an interaction coefficient. It is clear that this inter-particle force is repulsive at short range and attractive at long-distance. This inter-particle describes a volume force on continuum scale and can account for the formation of co-existing liquid–gas phases. The force obtained from Eq. (5) vanishes for interior particles in both liquid and gas phases, with small fluctuation around the overall direction of the macroscopic density gradient. For boundary particles, e.g., particles near the gas–liquid interface, a surface force is produced, pointing toward the denser phase. This IIF approach is comparatively simple and straightforward since it does not need to calculate the surface curvature, which is not an easy task for particle method such as SPH. One problem is that as the IIF model implicitly calculates the surface tension force with parameters from atomistic level, it needs parameter calibration, which relates the physical parameters from atomistic level to continuum level.

Another IIF model is to use some kind of equation of state, which can be used to close the equation system (4). An equation of state describes the relationship of the pressure p, density ρ, and the internal energy per unit mass e, respectively. For example, the vdW equation of state can be used to model the behavior of the fluid under consideration. The vdW equation of state was derived from statistical mechanics as the mean-field limit for the free energy density of a system of hard particles with a superimposed long-range and attractive pair potential. It is realistic to display a gas-to-liquid phase transition similar to that of a real fluid. The vdW equation of state can written as:

$$p = \frac{\rho \bar{k} T}{1 - \rho \bar{b}} - a\bar{\rho}^2 \tag{6}$$

and

$$e = \bar{k}T - \rho\bar{a}. \tag{7}$$

In the above two equations, $\bar{k} = k_B/T$, where k_B is the Boltzmann's constant. T is the system temperature. $\bar{a} = a/m^2$ and $\bar{b} = b/m$, where a and b are the parameters describing a vdW fluid. a controls the strength of the attractive force and b relates to the size of the particle.

The second part in Eq. (6) describes the cohesion among particles. Using SPH approximation for pressure and considering this cohesive pressure part separately, we can get:

$$\frac{D\mathbf{v}_i^\alpha}{Dt} = 2a\sum_{j=1}^{N} m_j \frac{\partial W_{ij}}{\partial \mathbf{x}_i^\alpha}. \tag{8}$$

It is clear that the attractive, long-range, and inter-atomic vdW force can be transformed into similarly attractive forces among SPH particles. Equation (8) describes a volume force on continuum scale to account for the formation of co-existing liquid–gas phases. This IIF model of using an equation of state to implicitly incorporate inter-particle interaction force does not need to locate the surface and then to calculate the local surface curvature. In addition, the surface tension is not a user-input parameter, while it is implicitly obtained from inter-particle interactions. If the particles are distributed regularly, the force obtained from Eq. (8) vanishes for interior particles in both liquid and gas phases. While for boundary particles, e.g., particles near the gas–liquid interface, since the inter-particle interaction force among different phases are generally different, a surface force is produced, which is basically perpendicular to the surface, pointing toward the dense phase. Nugent and Posch identified that to obtain acceptable results, a large influencing area (e.g., two times the smoothing length for approximating other field variables and the first part in Eq. (6)) is necessary to conduct the particle approximations in Eq. (8).

Figure 3(a) shows an example of using IIF model with vdW equation of state to model the large-amplitude oscillations of an initially oblate liquid drop. The initially oblate liquid drop with an aspect ratio of 5 was taken from a well-equilibrated circular drop. It is observed that the liquid drop underwent oscillations that closely resemble the oscillations of a large ball of water under micro-gravity conditions observed experimentally in the space shuttle Columbia.

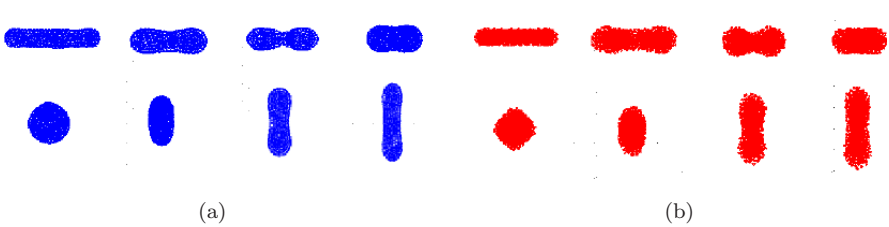

(a) (b)

Fig. 3. SPH (a) and DPD (b) simulations of a large amplitude oscillating droplet [Liu *et al.* (2006)].

The second approach is to incorporate the continuum surface force (CSF) model [Brackbill *et al.* (1992)] and introduced directly surface tension force into the momentum equation as expressed in Eq. (4). This approach is straightforward and physical parameters are used in the simulation. It is important to note that the surface tension parameters in this approach are user-input parameters and surface curvature needs to be calculated to get the surface tension force. Some researchers have used this approach in SPH method to model multiphase fluid flow [Morris (2000); Liu and Liu (2005)].

With this CSF model, the surface tension is added to the momentum equation as an external source force. The surface tension force F can be formulated as follows:

$$F = 2\gamma k(x) V \nabla V, \tag{9}$$

where γ is the surface tension coefficient, k is the surface curvature, and V is the volume of a fluid cell. Let n be the surface normal that can be computed from the gradient of the fluid cell as $n = \nabla V$, the surface curvature k is defined as

$$k = \nabla \cdot \hat{n} = \frac{1}{|n|}\left[\left(\frac{n}{|n|} \cdot \nabla\right)|n| - (\nabla \cdot n)\right], \tag{10}$$

where $\hat{n}$ is the unit surface normal defined as

$$\hat{n} = \frac{n}{|n|}. \tag{11}$$

For fluid cells near a solid wall, a wall adhesion model is applied to adjust the surface normal through using the contact angle θ, which is usually assumed to be constant in micro-channel flows with a small buck velocity, the dynamic contact angle can be assumed to be constant along the flow direction as the starting contact angle. The unit normal $\hat{n}$ is adjusted as follows for fluid cells close to the wall

$$\hat{n} = \hat{n}_w \cos\theta + \hat{n}_t \sin\theta, \tag{12}$$

where $\hat{n}_w$ and $\hat{n}_t$ are the unit vectors of the surface normal ($n = \nabla V$) and tangential to the wall, respectively. Thereby the unit surface normal $\hat{n}$ for fluid cells near the wall is adjusted using the contact angle. Whereas the unit surface normal $\hat{n}$ for fluid cells one cell away from the wall is normally calculated. After determination of the unit surface normal, the local surface curvature and, therefore, the surface tension can be calculated.

Figure 4 gives an example of CSF model in simulating micro-channel fluid flow. It is an underfill encapsulation process. The encapsulant is used to fill the space between the solder joints under the chip and the encapsulation process is either driven by a capillary action or by a pressurized injection [Liu and Liu (2005)].

4. Dissipative Particle Dynamics

DPD [Hoogerbrugge and Koelman (1992); Groot (1997)] is a relatively new meso-scale technique that can be used to simulate the behavior of complex fluids. In

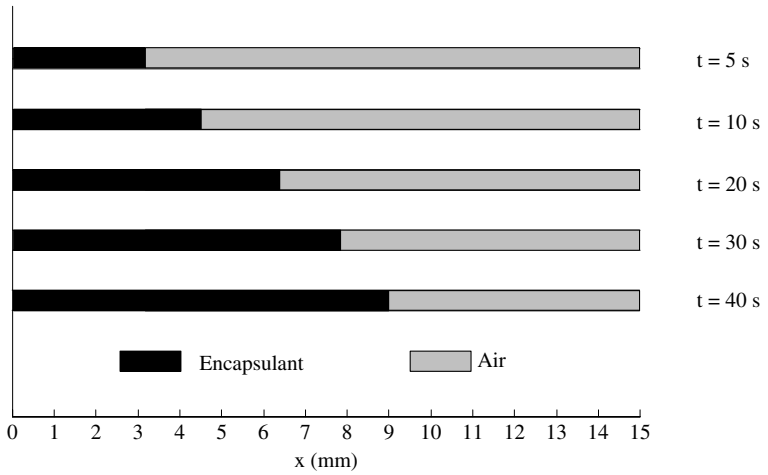

Fig. 4. Snapshots of the moving flow leading edge in an SPH simulation of a multiphase fluid flow in a micro-channel using the CSF model (from [Liu and Liu (2005)]).

DPD simulations, a complex system can be simulated using a set of interacting particles. Particles represent clusters of molecules that interact via conservative (non-dissipative), dissipative, and fluctuating forces. Because the effective interactions between clusters of molecules are much softer than the interactions between individual molecules, much longer time steps can be taken relative to MD simulations. A longer time steps combined with a larger particle size makes DPD much more practical to simulate hydrodynamics than MD. DPD is particularly promising for the simulation of complex liquids, such as polymer suspensions, liquids with interfaces, colloids, and gels. Because of the symmetry of the interactions between the particles, DPD rigorously conserves the total momentum of the system and because the particle–particle interactions depend only on relative positions and velocities, the resulting model fluids are Galilean invariant. Mass is conserved because the same mass is associated with each of the particles and the number of particles does not change.

It is convenient to assume that all of the particles have equal masses and use the mass of the particles as the unit of mass. Newton's second law governs the motion of each particle. The time evolution for a certain particle, i, is given by the following equation of motion:

$$\frac{d\mathbf{r}_i}{dt} = \mathbf{v}_i, \quad \frac{d\mathbf{v}_i}{dt} = \mathbf{f}_i = \mathbf{f}_i^{\text{int}} + \mathbf{f}_i^{\text{ext}}, \tag{13}$$

where $\mathbf{r}_i$ and $\mathbf{v}_i$ are the position and velocity vectors of particle i, $\mathbf{f}_i^{\text{ext}}$ is the external force including the effects of gravity, and $\mathbf{f}_i^{\text{int}}$ is the inter-particle force acting on particle i. The particle–particle interaction is usually assumed to be pairwise

additive and consist of three parts: a conservative (non-dissipative) force, $\mathbf{F}_{ij}^{C}$; a dissipative force, $\mathbf{F}_{ij}^{D}$; and a random force, $\mathbf{F}_{ij}^{R}$,

$$\mathbf{f}_i^{\text{int}} = \sum_{j \neq i} \mathbf{F}_{ij} = \sum_{j \neq i} \mathbf{F}_{ij}^{C} + \mathbf{F}_{ij}^{D} + \mathbf{F}_{ij}^{R}, \tag{14}$$

where $\mathbf{F}_{ij}$ is the inter-particle interaction force exerted on particle i by particle j, which is equal to $\mathbf{F}_{ji}$ in magnitude and opposite in direction. This symmetry of the interactions ensures that momentum is rigorously conserved. The pairwise particle interactions have a finite cutoff distance, r_c, which is usually taken as the unit of length in DPD models.

The dissipative force $\mathbf{F}_{ij}^{D}$ represents the effects of viscosity and is given by

$$\mathbf{F}_{ij}^{D} = -\gamma w^{D}(r_{ij}) \left(\hat{\mathbf{r}}_{ij} \cdot \mathbf{v}_{ij}\right) \hat{\mathbf{r}}_{ij}, \tag{15}$$

where γ is a coefficient, $\mathbf{r}_{ij} = \mathbf{r}_i - \mathbf{r}_j$, $\mathbf{r} = \mathbf{r}_{ij} = |\mathbf{r}_{ij}|$, $\hat{\mathbf{r}}_{ij} = \mathbf{r}_{ij}/\mathbf{r}_{ij}$, $\mathbf{v}_{ij} = \mathbf{v}_i - \mathbf{v}_j$ and $w^{D}(r_{ij})$ is the dissipation weight function. The random force $\mathbf{F}_{ij}^{R}$ represents the effects of thermal fluctuations and is given by $\mathbf{F}_{ij}^{R} = \sigma w^{R}(r_{ij}) \xi_{ij} \hat{\mathbf{r}}_{ij}$, where σ is a coefficient, $w^{R}(r_{ij})$ is the fluctuation weight function, and ξ_{ij} is a random variable. The fluctuation–dissipation relationship [Espanol and Warren (1995)] requires $w^{D}(r) = [w^{R}(r)]^2$ and $\gamma = \frac{\sigma^2}{2k_B T}$, where k_B is the Boltzmann constant and T is the temperature. One straightforward choice for the dissipative and random weight functions is $w^{D}(r) = [w^{R}(r)]^2 = (1-r)^2, r < 1$.

The conservative force, $\mathbf{F}_{ij}^{C}$, is a "soft" interaction acting along the line of particle centers and has the form $\mathbf{F}_{ij}^{C} = a_{ij} w^{C}(r) \hat{\mathbf{r}}_{ij}$, where a_{ij} is the magnitude of the repulsive interaction strength between particles i and j. For particles from different media, the strength coefficient can be different. $w^{C}(r_{ij})$ is the weight function for the conservative force. In previous DPD implementations, a conservative force weighting function in a simple form of $w^{C}(r) = 1 - r$ has been used. Because the fluid generated by DPD simulations with this purely repulsive conservative force is a gas, it cannot be used to simulate the flow of liquids with free surfaces, the behavior of bubbly liquids, droplet dynamics, and other important multiphase fluid flow processes. Including a long-range attractive component in $w^{C}(r)$ is necessary for such applications.

It is possible to construct a new particle–particle interaction potential $U(r)$ by combining the commonly used SPH cubic spline smoothing functions $W(r, r_c)$ with different interaction strengths A and B, and different cutoff distances r_{c1} and r_{c2}, multiplied by an interaction strength coefficient a

$$U(r) = a(AW(r, r_{c1}) - BW(r, r_{c2})). \tag{16}$$

The DPD conservative particle–particle interaction forces are thus given by $\mathbf{F}_{ij}^{C} = (-dU(r)/dr)\hat{\mathbf{r}}_{ij}$. The constructed interaction potential function $U(r)$ consists of short-range repulsive and large-range attractive interactions (when $A > B$ and $r_{c1} < r_{c2}$) and allows the behavior of gases, liquids, solids, and multiphase systems to be simulated. A certain set of parameters A, B, r_{c1}, and r_{c2} in Eq. (3)

determines the shape of the particle–particle interaction potential that describes the property of the corresponding fluid. The magnitude of the conservative force weight function and the location of the transition point from repulsion to attraction should be easily adjustable to allow the behavior of different fluids to be simulated [Liu *et al.* (2006)].

Similar to the IIF approach in the SPH in modeling surface tension, the modified DPD method allows surface tension to be modeled. For randomly distributed particles in a given DPD system, forces obtained using the new interaction potential (Eq. (16)) vanishes for interior particles in both liquid and gas phases. While for boundary particles, e.g., particles near the gas–liquid, since the inter-particle interaction force between different phases are generally different, a surface force is produced, which is basically perpendicular to the surface, pointing toward the dense phase. Figure 3(b) shows the large amplitude oscillation of a liquid drop using DPD method with such interaction potential [Liu *et al.* (2006)].

In DPD simulations, the effects of solid walls are usually be simulated by using fixed particles to represent the solid matrix near the solid–fluid interface. The nonslip boundary condition and contact line dynamics can be implemented by allowing solid particles to interact with fluid particles. By adjusting the fluid–solid and fluid–fluid interaction strength ratio a_w/a_f, it is possible to model different wetting effects. One example is to model the multiphase flow within two parallel plates. It is implemented by injecting DPD particles into the flat fracture with an interaction potential of $U(r) = a(2W_1(r, 0.8) - W_2(r, 1.0))$. By changing the interaction strength ratio a_w/a_f, injection rate, and gravity, the fluid flow within the fracture produces a rich variety of dynamic behaviors. The injected particle equilibrated with the particles that had previously entered the aperture and the wall particles and the injected fluid particles move to the right, further into the aperture, as the density of the injected particles and the concomitant pressure increased. A pressure drop along the fracture is produced due to the particle injection. The surface tension of the fluid is determined by the interplay between the attractive and repulsive components of the interaction between the fluid particles. The interaction between the wall particles and the fluid particles can be different from that between the fluid particles and these interactions can be tuned to give different wetting behaviors and capillary forces.

Figure 5(a) shows the particle distributions in the multiphase flow with an injection rate of 10 particles per 100 steps, $a_w/a_f = 10.0$ and $g = 0.02$. The fluid–wall

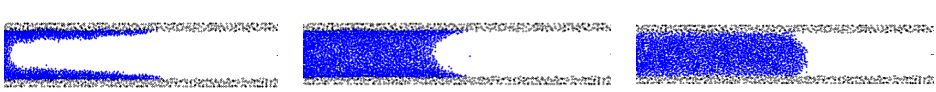

(a) (b) (c)

Fig. 5. Different wetting behaviors by changing the interaction strength ratio, from strong wetting (a) and moderate wetting (b) to non-wetting (c) effects.

interaction strength is much larger than fluid–fluid interaction strength and, therefore, the fluid demonstrates strong wetting effects. In Fig. 5(b), the injection rate was 100 particles per 100 steps, $a_w/a_f = 5.0$ and $g = 0.02$. The fluid–wall interaction strength is five times the fluid–fluid interaction strength and the flow is moderate wetting. Figure 5(c) shows the particle distributions in the multiphase flow with an injection rate of 100 particles per 100 steps, $a_w/a_f = 0.25$ and $g = 0.02$. Since the fluid–wall interaction strength is smaller than the fluid–fluid interaction strength, the contact angle is relatively large (obtuse angle) and the flow is non-wetting on the solid surface. In this simulation, the fluid propagates into the aperture with an approximately constant contact angle, which can be calculated from the shape of the advancing particle distributions. Again very few particles evaporated from the bulk flow. A larger injection rate or/and a smaller a_w ($a_w \geq a_f$) leads to a larger contact angle.

Figure 6 shows another example of multiphase flow in a cross fracture junction with a potential function of $U(r) = a(2W_1(r, 0.8) - W_2(r, 1.0))$, an injection rate of 100 particles per 100 steps, $a_w/a_f = 8$ and $g = 0.02$. It can be observed that before the junction, with the advancement of the fluid flow, DPD particle maintain a roughly constant advancing contact angle along the left channel with a strong wetting effects. When DPD particles arrive at the left corners of the cross junction, due to the strong wetting effects, DPD particles start to flow along the left side of

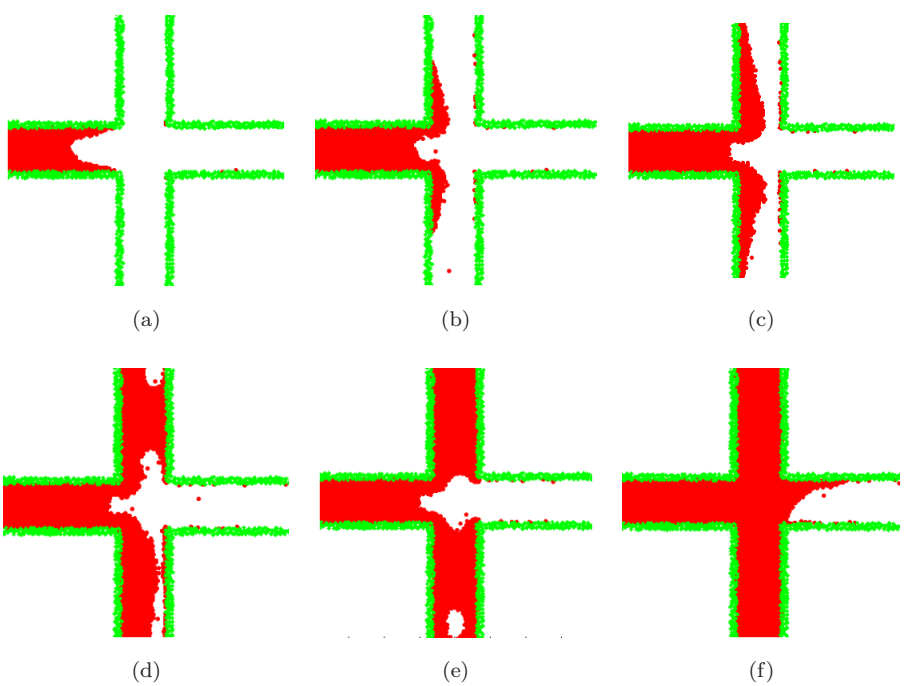

Fig. 6. Snapshots of multiphase flow in a cross fracture junction.

the top and bottom channels, where bulk flow will them form. It is noted that a gas bubble has been entrapped in the fluid liquid at the bottom channel. After the top and bottom channel haven been saturated, the flow start to propagate along the top side of the right channel, which demonstrates that in multiphase flow in fracture junction, there exists a preferential path along which the bulk liquid move faster. For above-mentioned two examples, the pressure drop, surface tension, and wetting behavior or capillary force, together with possible external forces, govern the fluid flow in the fracture, which may exhibit a rich variety of flow regimes.

5. Conclusions

In this article, we introduce SPH and DPD methods for multiphase flows with fluid–fluid–solid contact line dynamics. As Lagrangian particle methods, SPH and DPD models have special advantages over the traditional grid-based methods in modeling multiphase flows. They do not require explicit and complicated interface tracking algorithms and thus there is no need to explicitly track the material interfaces and the processes such as fluid fragmentation and coalescence can be handled without difficulty. They also do not require contact angle models since contact angles can be naturally inferred from the shape of the moving particle distributions and can vary spatially and temporally, depending on the dynamic balance of viscous, capillary, and gravitational forces.

There are two approaches in modeling surface tension and wetting behaviors in the SPH method based on CSF and inter-particle interaction force respectively, with each having its advantages and disadvantages. The CSF approach uses user-input parameters for surface tension, contact angle, and adhesion effects, but needs burdensome work to calculate the interface curvature. In contrast, the IIF approach does not need to calculate the interface curvature. Surface tension and wetting behavior are governed by the interaction of the inter particle (fluid–fluid and fluid–solid) interactions. Contact angle is no longer a user-input parameter as in the CSF model and can be obtained from measuring the concerned particle positions. In IIF model, some material properties need to be calibrated from the simulation process. The CSF model is more like the approaches used in continuum scale, conventional grid-based numerical methods for simulating multiphase dynamics, while the IIF approach takes a similar choice of inter-particle interaction as in the MD and DPD.

In IIF model (both in SPH and in DPD), fluid particles can move in open spaces within solid obstacles (fractures or porous media) and the interaction of fluid particles and solid particles can be used to study fluid–fluid–solid contact line dynamics and different wetting and spreading behaviors. The interaction strengths between the fluid particles and between the fluid and wall particles are closely related to the wetting behavior and the contact angles. A number of numerical examples with fluid–fluid–solid contact line dynamics have been studied using SPH and DPD models. It is revealed that multiphase flow with fluid–fluid–solid contact line dynamics is complicated due to the interplay of pressure drop, viscous,

capillary, and gravitational forces, geometry of solid obstacles, and the inflow conditions. The advancing and receding contact angles can vary spatially and temporally, depending on the dynamic balance of viscous, capillary, and gravitational forces.

Acknowledgments

This work has been supported by the National Natural Science Foundation of China (Grant No. 50976108, 10942004 and 11172306).

References

Brackbill, J. U., Kothe, D. B. and Zemach, C. [1992] A continuum method for modeling surface tension, *J. Comput. Phys.* **100**(2), 335–354.

Bracke, M., De Voeght, F. and Joos, P. [1989] The kinetics of wetting: The dynamic contact angle, *Trends Colloid Interf. Sci.* **III**, 142–149.

Chen, S. and Doolen, G. D. [1998] Lattice Boltzmann method for fluid flows, *Annu. Rev. Fluid Mech.* **30**, 329–364.

De Gennes, P. G. [1985] Wetting: Statics and dynamics, *Rev. Mod. Phys.* **57**(3), 827–863.

Espanol, P. and Warren, P. [1995] Statistical mechanics of dissipative particle dynamics, *Europhys. Lett.* **30**(4), 191–196.

Fang, H. S., Bao, K., Wei, J. A., Zhang, H., Wu, E. H. and Zheng, L. L. [2009] Simulations of droplet spreading and solidification using an improved SPH model, *Numer. Heat Tr. A-Appl.* **55**(2), 124–143.

Frenkel, D. and Smit, B. [2002] *Understanding Molecular Simulation: From Algorithms to Applications*, Academic Press, San Diego, CA.

Gingold, R. A. and Monaghan, J. J. [1977] Smoothed particle hydrodynamics-theory and application to non-spherical stars, *Mon. Not. R. Astron. Soc.* **181**, 375–389.

Groot, R. D. [1997] Dissipative particle dynamics: Bridging the gap between atomistic and mesoscopic simulation, *J. Chem. Phys.* **107**(11), 4423–4435.

Házi, G., Imre, A. R., Mayer, G. and Farkas, I. [2002] Lattice Boltzmann methods for two-phase flow modeling, *Ann. Nucl. Energ.* **29**(12), 1421–1453.

Hoogerbrugge, P. J. and Koelman, J. [1992] Simulating microscopic hydrodynamic phenomena with dissipative particle dynamics, *Europhys. Lett.* **19**, 155–160.

Inamuro, T., Ogata, T., Tajima, S. and Konishi, N. [2004] A lattice Boltzmann method for incompressible two-phase flows with large density differences, *J. Comput. Phys.* **198**(2), 628–644.

Li, Q., Cai, T. M., He, G. Q. and Hu, C. B. [2006] Droplet collision and coalescence model, *Appl. Math. Mech-Engl.* **27**(1), 67–73.

Liu, G. R. and Liu, M. B. [2003] *Smoothed Particle Hydrodynamics: A Meshfree Particle Method*, World Scientific, Singapore.

Liu, M. B. and Liu, G. R. [2005] Meshfree particle simulation of micro channel flows with surface tension, *Comput. Mech.* **35**(5), 332–341.

Liu, M. B., Liu, G. R. and Lam, K. Y. [2003a] Computer simulation of flip-chip underfill encapsulation process using meshfree particle method, *Int. J. Comput. Engrg. Sci.* **4**(2), 405–408.

Liu, M. B., Liu, G. R. and Lam, K. Y. [2003b] Constructing smoothing functions in smoothed particle hydrodynamics with applications, *J. Comput. Appl. Math.* **155**(2), 263–284.

Liu, M. B., Liu, G. R. and Zong, Z. [2008] An overview on smoothed particle hydrodynamics, *Int. J. Comput. Meth.* **5**(1), 135–188.

Liu, M. B., Meakin, P. and Huang, H. [2006] Dissipative particle dynamics with attractive and repulsive particle–particle interactions, *Phys. Fluids* **18**(1), 017101.

Morris, J. P. [2000] Simulating surface tension with smoothed particle hydrodynamics, *Int. J. Numer. Meth. Fl.* **33**(3), 333–353.

Nugent, S. and Posch, H. A. [2000] Liquid drops and surface tension with smoothed particle applied mechanics, *Phys. Rev. E* **62**(4), 4968–4975.

Rapaport, D. C. [2004] *The Art of Molecular Dynamics Simulation*, Cambridge University Press, Cambridge, UK/New York, NY.

Rothman, D. H. and Keller, J. M. [1988] Immiscible cellular-automaton fluids, *J. Stat. Phys.* **52**(3), 1119–1127.

Shan, X. and Chen, H. [1993] Lattice Boltzmann model for simulating flows with multiple phases and components, *Phys. Rev. E* **47**(3), 1815–1819.

Tartakovsky, A. and Meakin, P. [2005] Modeling of surface tension and contact angles with smoothed particle hydrodynamics, *Phys. Rev. E* **72**(2), 26301.

Thompson, P. A. and Robbins, M. O. [1989] Simulations of contact-line motion: Slip and the dynamic contact angle, *Phys. Rev. Lett.* **63**(7), 766–769.

Wu, X., Phan-Thien, N., Fan, X. J. and Ng, T. Y. [2003] A molecular dynamics study of drop spreading on a solid surface, *Phys. Fluids* **15**, 1357–1362.